Biomedical Signal Processing and Control 70 (2021) 102950

Contents lists available at ScienceDirect

Biomedical Signal Processing and Control

journal homepage: www.elsevier.com/locate/bspc

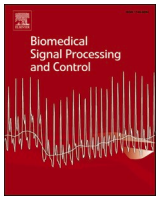

Automatic estimation of continuous elbow flexion–extension movement based on electromyographic and electroencephalographic signals

Valeria del C. Silva-Acosta, Israel Román-Godínez, Sulema Torres-Ramos, Ricardo A. Salido-Ruiz *

Computer Science Departament, Universidad de Guadalajara, Jalisco, Mexico

ARTICLE INFO

Keywords:
EEG
EMG
LSTM
Elbow joint angle estimation

ABSTRACT

The aim of this study was to estimate the elbow joint angle based on EMG and EEG signals using signal processing and machine learning techniques. 21 subjects (ten females, eleven males) performed synchronous flexion–extension movements while EMG, EEG, and elbow kinematic signals were recorded. The EMG and EEG signals were used to estimate the elbow angle employing a long short-term memory neural network. The best results were obtained by training one network per subject (intra subject). The lowest error was reached using the EMG signal, RMSE = 8.59°±2.17° and R^2 = 0.95 with a 95% CI (0.93–0.96). Employing EEG signals generated an RMSE = 9.27°±1.85° and R^2 = 0.95 with a 95% CI (0.94–0.95). When both signals, EMG/EEG, were used, the results were RMSE = 9.53°±2.13° and R^2 = 0.95 with a 95% CI (0.94–0.95). Statistically, for intra-subject data, there is no significant difference in RMSE on using a particular type of signal. In the case of inter-subject data, we obtained the lowest RMSE values considering the combination of EMG/EEG signals, for both, women and men, RMSE = 10.96°±5.28° and RMSE = 9.92°±4.62°, respectively. On the other hand, using subject-wise cross validation, errors increased as expected; however, men's EMG/EEG signals proved to be robust increasing the RMSE only in 3.47°. A new methodology is proposed for estimating elbow angles based on EMG and EEG biosignals. This can be useful for generating control signals for prostheses and/or exoskeletons designed to provide the support that people with motor disabilities require.

1. Introduction

According to the World Health Organization (WHO), about 15% of the world's population, over a billion people, live with some kind of disability, such as impairments, activity limitations, and participation restrictions [1]. Amputation, specifically, can be recognized as a disability since one of its main effects is reducing people's mobility. Amputation consists in removing all or part of a limb such as an arm, leg, or finger. Some 1.6 million amputations were performed in 2005 and this number is expected to double by the year 2050 [2]. To visualize the YLDs (Years lived with disability) due to amputation in 2019 considering both sexes, we used the GBD data visualization tool.[1]

Upper limb disabilities can occur as a consequence of numerous health conditions that belong to a wide range of categories, including tumors, chronic conditions (e.g. diabetes), complications of diseases, and injuries. Trauma is the main cause of upper limb amputations, representing 80% of such operations performed on men aged 15–45. Approximately 70% of upper limb amputations are performed below the elbow, with 10% occurring at the level of the hand or wrist [3]. In efforts to provide elbow amputees with instruments to restore mobility, several studies have used biosignals –specifically EMGs and EEGs– to estimate kinematic variables and then utilize these estimations as control signals for biomedical devices like prostheses and exoskeletons [4–11].

Kawase et al. [4] used EMG and EEG signals to control an upper limb exoskeleton, the angles of the metacarpophalangeal (MP) joint of the index finger, wrist, and elbow were estimated from EMG signals using a musculoskeletal model. Correlation coefficients were 0.81 ± 0.09, 0.85 ± 0.09, and 0.76 ± 0.13, respectively. On the other hand, Shing et al. [5] developed a mathematical muscle model based on anatomical and physiological data to estimate joint torque from EMG. Lalitharatne et al.

* Corresponding author.
E-mail address: ricardo.salido@academicos.udg.mx (R.A. Salido-Ruiz).

[1] YLD_figure in supplementary data shows the YLDs (Years lived with disability) due to amputation in 2019 considering both sexes, we used the GBD data visualization tool. Link: http://www.healthdata.org/gbd/data-visualizations.

https://doi.org/10.1016/j.bspc.2021.102950
Received 21 January 2021; Received in revised form 17 June 2021; Accepted 28 June 2021
Available online 24 July 2021
1746-8094/© 2021 The Authors. Published by Elsevier Ltd. This is an open access article under the CC BY license (http://creativecommons.org/licenses/by/4.0/).

[6] estimated the user's elbow joint angular velocity based on the EEG signals using a time-embedded linear model. Bandara et al. [10] identified the motion intention for arm reaching and hand lifting using classifiers trained with EEG features, the classifiers used were Multilayer Perceptron (MLP) and k-nearest neighbor. That work also estimated the elbow motion and hand endpoint using neural networks trained with shoulder angle. They achieved an accuracy of 73.7% in predicting motion intention for lifting and reaching motions of the upper limb.

Several techniques have been applied to estimate joint angles, such as filters (Wiener or Kalman), models of the musculoskeletal system, and machine learning, especially artificial neural networks (ANN).

Among the studies that have used ANN to estimate joint angles, Blana et al. [7] recorded six EMG signals from the area of the humerus, along with kinematic signals, to automate the control of a trans-humeral prosthesis. To do so, they trained a time-delayed artificial neural network (TDNN) that predicted elbow flexion–extension and forearm pronation-supination. Their results showed an error of $13^\circ - 23^\circ$ for these two movements. In addition, Blana et al. [12] performed a comparison of three different artificial neural networks (TDNN, LSTM, and ESN) using the same database as in their previous work [7]. The estimated movement was elbow flexion–extension and their results, in terms of the root mean squared error, were $11.80^\circ, 10.40^\circ$, and 16.30° for TDNN, LSTM, and ESN, respectively. Akhtar et al. [8] estimated the distal angles of the arm joint (elbow flexion–extension, forearm pronation-supination) using EMG signals and shoulder orientation for trans-humeral prostheses. They applied an adaptive neural network (TDANN) with the locally-weighted projection-regression algorithm (LWPR), obtaining determination coefficients of 0.72 for flexion–extension movements and 0.82 for pronation-supination. In the same year, Grech et al. [9] estimated four single-joint movements and three simultaneous movements based on EMG signals. The former included flexion–extension, shoulder flexion–extension, shoulder horizontal adduction-abduction, and shoulder vertical adduction-abduction. The latter movements were shoulder and elbow flexion–extension and elbow flexion–extension with horizontal and vertical adduction-abduction. Their work employed three different artificial neural networks: the multilayer perceptron (MLP), a time-delay neural network, and a recurrent neural network (RNN), to estimate these movements. The determination coefficients obtained for elbow flexion–extension was 0.74 for the MLP algorithm, 0.79 for the TDNN network, and 0.78 for RNN.

Chen et al. [11] proposed a method for controlling trans-humeral prostheses using both EEG and EMG signals. The latter were employed to control elbow extension/flexion, and the regression method applied was a back propagation neural network (BPNN). The EEG signals were used to classify four different hand motions, while steady state visual evoked potentials (SSVEP) were utilized to extract features from the signals, and the canonical correlation analysis (CCA) algorithm classified the SSVEP signals. The accuracy reported in their classification task ranged from a minimum of 60% to a maximum of 100%. The studies that estimated elbow joint angle by applying artificial neural networks (Blana et al. [7], Akhar et al. [8], and Grench et al. [9]) used only EMG signals, while Chen et al. [11] used both EMG and EEG signals, though only the former were applied to estimate elbow flexion/extension, as the latter were processed to classify the four hand movements.

EMG signals are the ones most often used because they are closely-related to movement. Not all subjects, however, are candidates for the use of this technique. It is not possible, for example, to obtain EMG signals from the arm muscles of people with shoulder dis-articulation (*i.e.*, amputation of the entire arm). Another case is that of people who present muscular atrophy. This makes it necessary to obtain an alternative source of information to estimate kinematic variables. One option is EEG signals since they can be recorded from virtually all people. However, to the best of our knowledge, the elbow flexion/extension estimation studies carried out to date have not considered these signals. Another factor may be that EMG signals are influenced by gender [13], and the studies mentioned above present only inter-subject results, so this potential influence has not yet been considered.

The present study, therefore, was designed to estimate elbow joint angle values using both EMG and EEG signals, first separately, and then combined. All signals were acquired during synchronous upper limb mobility protocols in healthy subjects. Experiments that considered both inter-subject and intra-subject results in women and men were conducted to analyze performance in every case. The angle estimations were calculated by implementing a long short-term memory artificial neural network in an effort to improve state-of-the-art performance.

2. Materials

2.1. Features

Signals can be characterized in the time and frequency domains, among others. The features that showed relevant information regarding upper limb kinematics from the EMG and EEG signals are presented, beginning with the time domain features.

Time domain features are shown next.

2.1.1. Mean

The mean of a discrete signal $\mathbf{x}$, is the average value defined by Eq. (1):

$$\bar{x} = \frac{1}{N}\sum_{i=1}^{N} x_i \tag{1}$$

where $N \in \mathbb{N}$ is the number of samples of the discrete signal, x_i is the i^{th} value of $\mathbf{x} \in \mathbb{R}$, and $\bar{x} \in \mathbb{R}$ is the average value of the discrete signal [14].

2.1.2. Zero crossing

Zero crossing (ZC) is the number of times the signal values cross the zero amplitude value [15]. To avoid low-voltage fluctuations or noise, a threshold is considered. The mathematical expression is defined in Eq. (2):

$$ZC = \sum_{i=1}^{N-1} f(x_i, x_{i+1}) \tag{2}$$

$$f(v,w) = \begin{cases} 1, & \text{if } [(v > T) \wedge (w < T)] \vee [(v < T) \wedge (w > T)] \\ 0, & \text{otherwise} \end{cases}$$

$$T = 4\left(\frac{1}{10}\sum_{i=1}^{10} x_i\right)$$

where $N \in \mathbb{N}$ is the number of samples, x_i is the i^{th} value of the discrete signal $\mathbf{x} \in \mathbb{R}$, and x_{i+1} is the following discrete value.

2.1.3. Waveform length

Waveform length (WL) measures the complexity of the signal, defined as the cumulative length of the signal waveform in a time segment [16]. The mathematical expression is shown in Eq. (3).

$$WL = \sum_{i=1}^{N-1} |x_{i+1} - x_i| \tag{3}$$

where $\mathbf{x} \in \mathbb{R}$ is the discrete signal, x_i is the i^{th} value of $\mathbf{x}$, and x_{i+1} is the following value, and $N \in \mathbb{N}$ is the number of samples in the discrete signal.

2.1.4. Slope sign change

As its name suggests, this is the number of times the slope of a signal changes its sign. The number of changes between positive and negative slopes in three consecutive segments was calculated using a threshold to avoid signal noise. Slope sign change (SSC) is defined in Eq. (4) [17].

$$SSC = \sum_{i=2}^{N-1} f(x_i, x_{i-1}, x_{i+1}) \tag{4}$$

$$f(x_i, x_{i-1}, x_{i+1}) = \begin{cases} 1, & \text{if } \begin{array}{c}[(x_i > x_{i-1}) \wedge (x_i > x_{i+1})] \quad \vee \\ [(x_i < x_{i-1}) \wedge (x_i < x_{i+1})] \quad \wedge \\ (abs(x_i - x_{i+1}) \geqslant T)] \quad \vee \\ [abs(x_i - x_{i-1}) \geqslant T] \end{array} \\ 0, & \text{otherwise} \end{cases}$$

where x_i is the current value of the discrete signal $\mathbf{x} \in \mathbb{R}$, x_{i+1} is the next value, and x_{i-1} is the previous one; $T = 0.01$, and *abs()* represent the absolute value.

The frequency and time-scale features are presented below.

2.1.5. Power spectral density

Power spectral density (PSD) is an important metric in frequency domain analysis [16]. The PSD of the function $x(m)$ is defined as the Fourier Transform of the autocorrelation function of the signal $x(m)$. It is defined in Eq. (5).

$$PSD = \sum_{m=-\infty}^{\infty} r_{xx}(m) e^{-j2\pi fm} \tag{5}$$

where m is a real variable, $r_{xx}(m)$ is the autocorrelation function of $x(m)$, f is the frequency, and j is the square root of -1.

2.1.6. Wavelet transform

The discrete wavelet transform (DWT) uses filter banks to construct a multi-resolution time–frequency plane. A filter bank consists of filters that separate the signal into different frequency bands represented by wavelet coefficients [18].

The decomposition of signal S at level i consists of approximation coefficients A_i and detail coefficients from level 1, D_1, up to level i, D_i.

The mean of the detail coefficients from levels 4 to 7, and the approximation coefficients of level 7 were considered. These levels were selected because they include low frequencies, and previous studies have demonstrated that these are the frequencies that contain information about upper limb kinematics in EEG signals [19].

2.2. Neural networks

2.2.1. Long short-term memory

One type of neural network designed to manage time-series forecasting is the recurrent neural network (RNN). RNNs are commonly used to model dynamic systems and have the specific feature of sending feedback signals. They are, however, susceptible to the vanishing gradients problem because they retro-propagate the gradients through several layers [20]. For this reason, long-short term memory (LSTM) networks were created. The main advantages of LSTMs are that they introduce memory (or cell) information, and are free from the vanishing gradients problem [21]. The central concept of LSTM is the memory (or cell) unit c_t, which encodes the information from the inputs observed up to a certain moment. The memory cell, c_t has the same inputs (h_{t-1} and x_t) and outputs (h_t) as a common recurrent network, but contains more gates to control the information flow. The input and output gates control data entry into the memory cell, and the information processed by the unit, respectively. The forget gate decides the information that is to be retained or neglected.

2.2.2. Loss function

This function is used to evaluate a learning model (*i.e.*, a set of weights). It is also known as the loss, or objective, function.

The common loss functions used in regression problems are mean absolute error (*MAE*) and root mean square error (*RMSE*). Here we use *RMSE* and it is defined by Eq. (6).

$$RMSE = \sqrt{\frac{1}{n} \sum_{i=1}^{n} (y - \widehat{y})^2} \tag{6}$$

Where $n \in \mathbb{N}$ is the number of examples or instances considered, y is the target value and $\widehat{y}$ is the estimated value.

2.3. Model validation

2.3.1. Cross-validation

Cross-validation is a widely-used method to assess the performance of learning models. In this method, the initial data is divided into $k \in \mathbb{N}$ disjoint folds of the same size (except for the final one), $D_1, D_2, \ldots, D_k$. Then, in the iteration $i \in \{1,2,3,\ldots,k\}$, fold D_i is used to test the model, while the others are used to train it. In this methodology, each fold is used $k-1$ times as a training set and once as a test set [22].

In the case of stratified cross-validation, each subset has approximately the same class distribution as the original dataset.

2.3.2. Coefficient of determination

The coefficient of determination, R^2, can be interpreted as the portion of the total variation that is explained by the regression model [23]. The mathematical expression of R^2 is shown in Eq. (7).

$$R^2 = 1 - \frac{\sum (y - \widehat{y})^2}{\sum (y - \bar{y})^2} \tag{7}$$

2.3.3. Confidence intervals

Confidence intervals (CI) are a very helpful tool to describe analyses of research data [24]. CI are defined by Eq. (8).

$$CI = \overline{X} \pm z * \frac{s}{\sqrt{n}} \tag{8}$$

Where $\overline{X}$ is the sample mean, z the confidence level value, s the sample standard deviation and n are the sample size.

3. Methods

The methodology proposed for estimating motion intention is shown in Fig. 1. The biosignals used to make these estimations are EMG and EEG recordings, as shown in the upper section of the figure, while the bottom section presents the measured angular displacement that is to be estimated (*i.e.*, angular value of the elbow joint) employed only in the training stage of the LSTM. The biosignals were first recorded, then preprocessed (filtered, aligned, segmented). Later, the EMG and EEG features were extracted and those features and the respective angular displacement of the elbow joint are used together to build the dataset utilized to construct the model and then evaluate it. Finally, the EMG and EEG features were used to estimate the elbow angle. The following sections present, in greater detail, each step of our proposed methodology.

3.1. EMG/EEG data aquisition

3.1.1. Participants

All signal recordings were acquired following the protocol accepted on July 6th, 2020, by the Research and Ethics in Research Committees of the Centro Universitario de Ciencias de la Salud at the Universidad de Guadalajara (folio number 20–86). EMG and EEG signals were recorded from 21 subjects, ten females and eleven males, in an age range of 18–25 years. No subjects had neuromuscular pathologies that affected their right arms. They all received detailed written and spoken information about the protocol and any doubts were clarified. All participants signed a form to confirm their consent to participate.

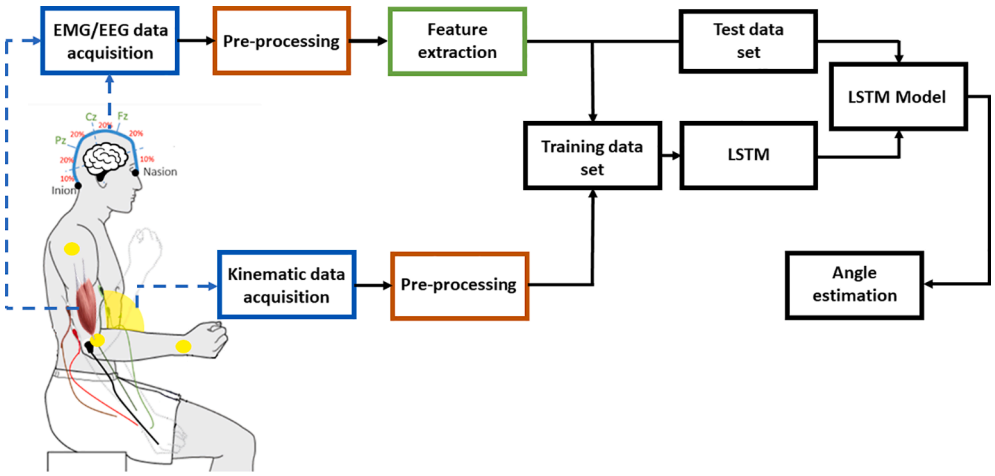

Fig. 1. Proposed approach for estimating motion.

3.1.2. Synchronous mobility protocol

This protocol consists of a series of flexion–extension movements executed by the right arm. During these movements, subjects were seated, looking straight ahead at a screen with their arm extended in an intermediate position of pronosupination.

While receiving the instructions via a video, and before making the first movement, subjects were asked to keep their arms extended. The test began with a flexion movement that lasted 1.5 s. While flexed, the arm was maintained in an isometric position for 3 s. At that point, subjects began the extension of their arms in a movement that took 1.5 s. Finally, the arm was maintained in an isometric position for 3 s. Each subject was asked to perform this routine 10 times, receiving assistance throughout the test. All instructions and movements were displayed in real time as shown in Fig. 2.

3.1.3. Experimental setup

A GRASS Comet biosignal amplifier was used to acquire the muscular and neural signals. EMG recordings of the biceps brachii and triceps brachii were done by setting a bipolar configuration, an inter-electrode center-to-center distance (IDE) of 40 mm was chosen by following the SENIAM (seniam.org) recommendations. For the EMG recording, we apply alcohol to cleanse the skin and use 10 mm disc gold (Au) electrodes aligned with muscle fibers. To guarantee proper electrode–skin contact we apply highly-conductive paste. One electrode was placed on the belly of each muscle while a second electrode was placed on the distal tendon of the corresponding muscle. The reference electrode was placed on the elbow since there is low to null electrical activity.

The standard EEG 10 −20 system was followed using 19 electrodes placed at the F8, F3, F4, T3, T4, C3, C4, T5, T6, P3, P4, O2, O1, FZ, CZ, PZ, A1, A2 positions. The reference electrode was placed at the inion. In these experiments, an electrode cap was used to record the EEG signals with conductive gel applied to obtain the desired impedance (less than 10$K\Omega$). A sampling rate of 400 Hz was chosen, considering that was the maximum sampling rate frequency of the available acquisition equipment and also because some studies have reported good performances using a sampling rate of 400 Hz for addressing problems like muscle activity decoding [25] and on studying the effect of the sampling rate variation on classification performances for a hand motion recognition problem [26].

Angular displacement of the elbow joint was measured to evaluate

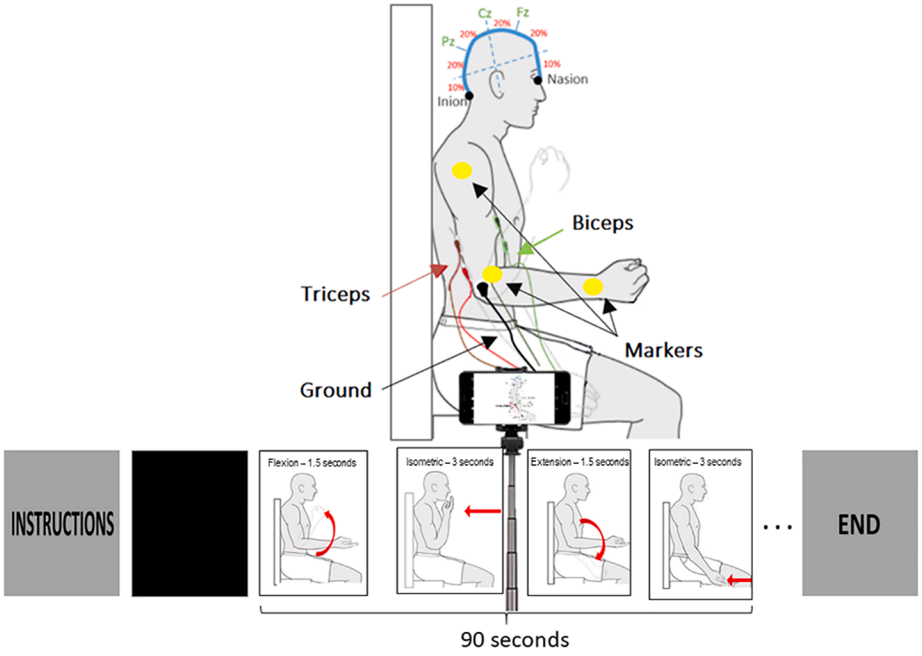

Fig. 2. Assembly of the instruments and sensors for the synchronous mobility protocol of the upper limb and frames of the instructions presented.

LSTM estimations. To achieve this, three markers were placed on the right arm, one on the upper arm, the second on the elbow, and the third on the forearm at the level of the wrist for video-processing. This was done using Kinovea software in order to obtain the angles of the elbow during displacement. Kinovea is an open-source motion analysis software that aims to study human motion: capture, observation, annotation, and measurement. Kinovea uses the markers placed on the arm to construct segments around a joint (central marker); these segments perform an angular displacement around the joint changing the angle between them. The angular value is calculated by kinovea frame by frame for the whole captured motion using basic trigonometric functions. For recording, a camera was set up in front of the markers to record the flexion–extension movements of subjects' arms. The camera captured videos at 60 frames per second. The placement of the sensors and instruments are shown in Figs. 3 and 4. All the files generated by the recording signals are found in Supplementary Data Material.

3.2. Data pre-processing

The raw EMG signals contained movement artifacts marked by low frequencies and high amplitudes. For this reason, after centering the signals, a fifth-order FIR bandpass filter between 5 −65 Hz was applied [27], the filter uses a least-squares approximation to compute the filter coefficients and then smooths the impulse response with a Hamming window. The signal was centered by subtracting the overall mean, to exclude the DC offset component, keeping the signal centered at zero.

A point-to-point comparison between the observed angular displacement captured by video, and electrophysiological activity is needed not only to train the learning model but also to measure any errors between the measured angular displacement and its estimation. Thus, in order to match the sampling rate to the EEG and EMG signals, the angular signals were re-sampled at 400 samples per second after a one dimensional median filtering was applied to smooth signal variations. The EMG and EEG signals were then aligned with the kinematic signal. To accomplish this, the cross-correlation between the EMG and EEG signals and the kinematic signal was measured, and alignment was made at the point of highest correlation.

The EMG and EEG signals were segmented into the four movements performed by subjects (flexion, isometric flexion, extension, isometric extension). The signal from each movement was divided into 10 windows. As a result we have 10 epochs of variable width for every movement to maintain the same number of instances per subject.

Fig. 3. Assembly of the instruments and sensors for the synchronous mobility protocol of the upper limb.

Fig. 4. GRASS Comet biosignal amplifier.

Stationarity is captured through the LSTM by varying the time-steps by 40 (one movement cycle) and 80 (two movement cycles) prior.

After that, the fact that we had already aligned the EEG/EMG and kinematic signals allowed us to construct several tuples with signal segments and angles (window, angle). In what follows, each tuple will be called an *instance*. As a result, each movement has 10 instances which generate 40 instances per movement cycle and 400 instances for all repetitions by each subject. These instances, specifically the signal segments, were then processed to compute the several features that were used to build the datasets to train and then test the LSTM model.

The following section presents the feature extraction methods used to compose the pair (feature-vector, angle).

3.3. Features extraction

Feature extraction and selection are two essential techniques used to achieve high-quality performance on estimation tasks when applying machine learning techniques. To perform this step, several features from the EMG and EEG signals were extracted in the time, frequency, and time-scale domains, as described in Section 2.

For EMG in the time domain, we extracted the mean, ZC (zero crossings) considering a threshold of 1 mV, WL (wavelength), and SSC (number of sign slope changes) at a threshold of 1 mV. This threshold was chosen to avoid low-voltage fluctuations [16]. These features have proven to be suitable for describing the movement of the elbow joint. In the present study, they were extracted from the biceps signal since its muscular activation shows a greater relation to the angular movement than the triceps signal [28].

In the case of the EEGs, features were extracted in both the frequency and time-scale domains. In the former, the signal mean power in the range of 0.3 −3 Hz was extracted from the power spectrum density. Low frequencies were chosen because they are appropriate for describing upper limb kinematics from EEG signals [19]. In the latter (discrete wavelet transform), we extracted the mean of the detail coefficients from levels 4 −7 and the approximation coefficients of level 7. For decomposition, we used 5^{th}-order wavelet from the Daubechies family (db5). Channels C3, C4, and CZ were selected for feature extraction from 10/20 system, because these electrodes were placed on the motor cortex, as shown in earlier studies [29–32].

3.4. Motion estimation

Estimations of the angular values of the elbow joint based on the EMG and EEG signals were performed using an LSTM network. The batch size selected was 10 instances. The LSTM contained a hidden layer

with 20 cells. The total number of epochs was 50. The solver used was ADAM with the following settings: $\alpha = 0.001, \beta_1 = 0.9, \beta_2 = 0.999, \epsilon = 1e^{-07}$. The algorithm was optimized based on mean absolute error. The time steps were 40 and 80, considering that each set of 40 instances represented one complete movement cycle (flexion, isometric-flexion, extension, isometric-extension). At the end of the LSTM layers, a dense neural network was appended with only one neuron and the identity function as the activation function.

3.5. Evaluation of the model

Evaluation of the LSTM was conducted using two approximations of the K-fold cross-validation methodology, record [22] and subject-wise [33,34]. To do so, the value of k was calculated dividing the total of instances in a dataset by the number of instances in one flexion–extension movement. For instance, in intra-subject experiments, each dataset has 400 instances, from which every 40 consecutive instances complete one flexion–extension movement; hence, k is equal to 10. On the other hand, in inter-subject experiments, each dataset has 4000 instances with the same number of instances per flexion–extension movement as intra-subject experiment; therefore, k is equal to 100. There is, however, an extra consideration in the calculation of k; the time step parameter. In this sense, the LSTM requires a particular accommodation of the dataset, this is, it is necessary to append the attributes of one or several previous instances to the next one to take advantage of the memory capability of the LSTM; resulting on a reduction of the training an testing dataset which in consequence affects the value of k. For instance, when 40 timesteps were used, the intra-subject dataset size was reduced to 360 instances per subject, while using 80 timesteps reduced the dataset to just 320 instances.

4. Results

Three experiments were designed to discern the advantages or disadvantages of using EMG and EEG signals on an automatic estimation task, both independently (EMG, EEG) and combined (EMG/EEG). To do so, several datasets were created. First, one dataset per subject was used to build an equal number of LSTM models (intra-subject). Next, two additional datasets were created, one with data from the women only, the other with data only from the men (inter-subject). As a result, an equal number of LSTM models were trained. The performance of the models was measured by calculating the *RMSE* and the determination coefficient, R^2. From this point forward the LSTM models will be referenced as VISR-Estimator.

The performance scores of the LSTM model for the intra-subject angle estimations are shown in Table 1 in the form of means, standard deviations, minimum and maximum values of the *RMSE*, along with the mean of the R^2 and its confidence interval (CI) of 95%. The table is organized by signal type and the previous timesteps. The best result for each signal is highlighted in black.

Clearly, for the 40 timesteps intra-subject data, the *RMSE* of the EMG signals presents a wider range of variation than the one for EEG signals and the combination EMG/EEG. The latter having the lowest STD. In contrast, for the 80 time-step intra-subject data, the RMSE obtained for EEG signal had the lowest STD. Table 2 shows the results of a pairwise signal ANOVA, we can see that there were no significant differences in the performance averages among the EMG, EEG, and EMG/EEG approaches for either the 40 or 80 time-step data.

In addition, an inter-subject data experiment was performed by grouping the instances by signal and gender. Table 3 shows the average *RMSE* along with the R^2 average and its CI 95% for 40 and 80 timesteps. The lowest *RMSE* values for the inter-subject women and men are highlighted in black.

Based on the results in Table 3, which indicate that the best estimations are those using EMG/EEG signals for men and women with 80 timesteps, we decided to conduct an ANOVA to determine whether there were any significant differences between using the EEG or the EMG/EEG signals.

Table 4 shows significant differences in RMSE performance for women using EEG and EMG/EEG, as well as between women using EEG and men using EEG or EMG/EEG. Three out of four combinations presented significant differences (p-value < 0.01) in the RMSE performance values (highlighted in black). Note that RMSE obtained from women's EEG are significantly different from RMSE obtained by women's EMG/EEG, also RMSE obtained from men's EEG are significantly different from RMSE obtained by men's EMG/EEG and finally there are significant differences in RMSE obtained between women and men when using EEG.

The following two conditions fit the inter-subject data; first, it contains several instances per subject, and second, it is organized by signal and gender. Hence, it was decided to follow a subject-wise cross-validation strategy to validate the results. Table 5 shows the average *RMSE* and the average R^2 along with its CI 95% for 40 and 80 timesteps. The lowest *RMSE* values for the inter-subject women and men are highlighted in black. Observe that in both validation strategies, the best results are presented in the EMG/EEG signal but on different time-step, 40 for record-wise and 80 for subject-wise. In addition, it is important to note that the *RMSE* increases for women –12.43° (40 timesteps) and 18.4° (80 timesteps)– and for men –3.47° (40 timesteps) and 14.8° (80 timesteps)–.

To obtain a graphical visualization of the estimations of performance, Fig. 5 depicts the angular displacement expected with the estimated EMG, EEG, and EMG/EEG values. Those values, both expected

Table 2
P-values and F-scores obtained for intra-subject data

Signals	Timesteps	*F*-value	*p*-value
EMG vs. EEG	40	1.57	0.21
	80	1.90	0.17
EMG vs. EMG/EEG	40	0.97	0.31
	80	1.98	0.16
EEG vs. EMG/EEG	40	0.30	0.58
	80	0.02	0.89

Table 1
RMSE values and average R^2 for intra-subject data.

Signals	Time-steps	Folds(k)	***RMSE*** (Degrees)				R^2	
			MEAN	STD	MIN	MAX	MEAN	95% CI
EMG	40	9	10.59°	4.44°	5.95°	23.58°	0.92	0.90–0.93
	80	8	**8.59°**	**2.17°**	5.76°	13.39°	0.95	0.93–0.96
EEG	40	9	**9.27°**	1.85°	5.05°	12.05°	0.95	0.94–0.95
	80	8	9.44°	**1.81°**	6.6°	15.14°	0.95	0.93–0.96
EMG/EEG	40	9	9.57°	**1.64°**	5.57°	13.1°	0.95	0.94–0.95
	80	8	**9.53°**	2.13°	6.42°	13.95°	0.95	0.94–0.95

In bold are presented the lowest mean and standard deviations of RMSE (degrees) for each one of the tested signals.

Table 3
Results obtained by LSTM trained with inter-subject data using record-wise cross validation.

Signals	Data arrangement	Timesteps	Folds	RMSE mean (Degrees)	STD	R2	CI
EMG	Women	40	99	21.18°	9.37°	0.76	0.70–0.81
		80	80	19.57°	7.55°	0.79	0.74–0.83
	Men	40	109	14.11°	9.19°	0.89	0.86–0.91
		80	108	14.06°	8.33°	0.88	0.85–0.90
EEG	Women	40	99	14.45°	7.89°	0.9	0.88–0.91
		80	80	14.51°	6.74°	0.91	0.89–0.92
	Men	40	109	13.38°	6.67°	0.9	0.88–0.91
		80	108	11.82°	5.12°	0.91	0.89–0.92
EMG/EEG	Women	40	99	12.68°	8.51°	0.92	0.90–0.93
		80	80	10.96°	5.28°	0.93	0.91–0.04
	Men	40	109	10.85°	6.56°	0.94	0.92–0.95
		80	108	**9.92°**	**4.62°**	0.94	0.92–0.95

Table 4
P-values and F-scores obtained for inter-subject data

Signals	*F*-value	*p*-value
Women EEG vs. Women EMG/EEG	16.89	**5.83** e^{-05}
Women EEG vs. Men EEG	9.20	**0.0027**
Women EMG/EEG vs. Men EMG/EEG	2.25	0.11300
Men EEG vs. Men EMG/EEG	6.85	**0.0095**

and estimated, correspond to the average of the expected and estimated values of the intra-subject test data for all 21 subjects. The red, blue, and pink solid lines are the estimated values from the EMG, EMG-EEG, and EEG signal, respectively, the black line indicates the expected value. The dotted lines are the mean ± STD of estimated angles. These estimations were made using the LSTM and considering 80 timesteps. Note that the inflection zones are where the estimates are more erratic, but where the slope is maintained the estimates are more accurate.

Table 6 presents an intra-subject comparison with the state-of-the-art. In the reported cases, elbow flexion–extension estimations were performed using the EMG signals with some use of additional signals, such as elbow orientation and humerus acceleration. This Table shows, for each phase of the study, the number of subjects used in the experiments, the model trained, and the average *RMSE* along with the R^2 coefficient and CI 95% of the R^2. At the end of the Table, our proposal is shown, based on the results of our experiments. Note that in our study a higher number of subjects performed the experiments, and our results outperform those from previous works.

Finally, a simulation of the elbow flexion–extension movement was performed using the information from male subject #5 (chosen arbitrarily) and the LSTM model trained with the EMG signal and 80 timesteps. This involved using OpenSim [35], and the model of the upper limb musculoskeletal system developed by Chadwick et al., [36] called "dynamic arm simulator". This model was chosen because it permits simulating arm dynamics in real time. A simulation video is available in Supplementary Multimedia Material.

The results from the simulation show that it is feasible to recreate the elbow flexion–extension movement from the EMG and EEG signals using the LSTM network. Also, we verified that the moment where the estimation has the highest error is when changing from one movement to another.

4.1. Discussion

Before discussing the main results of this work, it is important to clarify some aspects of the recorded signals used in this study. Both EEG and EMG signals were recorded with the same equipment (GRASS Comet biosignal amplifier) at the same sampling rate of 400 Hz; this has some advantages concerning data processing resources. However, it has also some controversial implications concerning the recommended sampling frequency for EMG signals acquisition. In our defense without loss of generality we can say that conclusions of this work remains unchanged because several studies [25,26] have shown that an EMG sampling frequency of 400 Hz reaches a comparable performance to higher frequencies of 1 kHz. In [25], a motor intention decoding scheme suitable for low frequency EMG signal is proposed and in [26] the authors presents an exploration of the relation between EMG Sampling Frequency and Hand Motion Recognition Accuracy, concluding that an "appropriate reduction of the sampling frequency can be a good choice

Table 5
Results obtained by LSTM trained with inter-subject data using subject-wise cross validation

Signals	Data arrangement	Timesteps	Folds (k)	RMSE mean (Degrees)	R^2	CI
EMG	Women	40	10	33.62°	0.45	0.70–0.81
		80	10	39.57°	0.17	0.74–0.83
	Men	40	11	25.03°	0.70	0.86–0.91
		80	11	33.22°	0.47	0.85–0.90
EEG	Women	40	10	28.10°	0.57	0.88–0.91
		80	10	36.62°	0.40	0.89–0.92
	Men	40	11	25.90°	0.62	0.88–0.91
		80	11	40.06°	0.16	0.89–0.92
EMG/EEG	Women	40	10	**25.11°**	0.66	0.90–0.93
		80	10	29.36°	0.59	0.91–0.04
	Men	40	11	**14.32°**	**0.91**	0.92–0.95
		80	11	24.72°	0.70	0.92–0.95

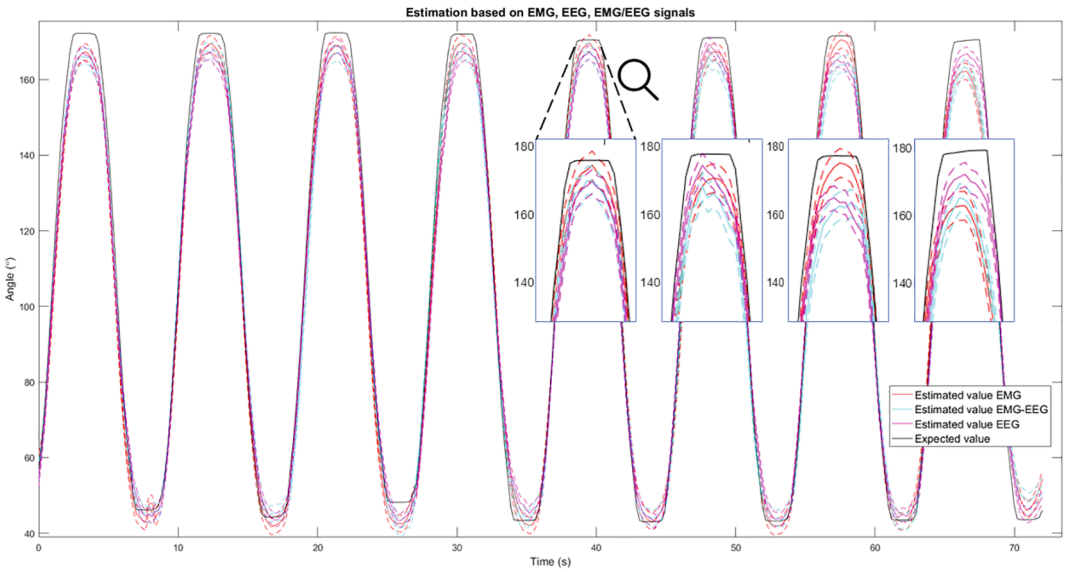

Fig. 5. Expected and estimated elbow angle based on the EMG, EEG and EMG/EEG signals.

Table 6
Comparison with studies that estimate elbow flexion–extension

Author	Signal	Channels	Sampling rate	Subjects	Model	Results	
						RMSE	R^2
Blana et al. 2016	EMG HA	6 3	1000 Hz	10	TDNN	13.70°	–
Ahkatar et al. 2017	EMG SO	13 3	1000 Hz	8	LWPR TDANN	12.38° 12.79°	0.61 0.58
Grench et al. 2017	EMG	5	1000 Hz	5	MLP TDNN RNN	16.34° 15.39° 14.7°	0.74 0.79 0.78
Blana et al. 2020	EMG HA	6 6	1000 Hz	10	TDNN LSTM ESN	11.80° 10.40° 16.30°	– – –
VISR-Estimator	EMG EEG EMG/EEG	1 3 4	400 Hz	21	 LSTM	**8.59°** **9.44°** **9.53°**	**0.95** **0.95** **0.95**

HA* is for humerus acceleration, SO** is for shoulder orientation.
Time delay neural network (TDNN).
Locally Weighted Projection Regression (LWPR).
Multilayer Perceptron (MLP).
Recurrent Neural Network (RNN).
Long Short-Term Memory (LSTM).
Echo State Network (ESN).

to balance the cost and performance of a multiple channel EMG system for feature-based hand gesture classification". Considering that hand gesture classification is a harder task than elbow flexion/extension, presented in this study, we believe that our results are consistent with the test presented here.

Regarding the results obtained for processing the intra-subject data and analyzing the experiment in which LSTM was trained setting its timesteps to 40 and with EMG as the input signal, the resulting model presented the worst performance of all the signals tested (see Table 1), with an average *RMSE* and standard deviation error of 10.59°, and 4.44°, respectively. However, using the EEGs or EMG/EGGs as the input signals helped reduce the standard deviation error to 1.85° and 1.64°, respectively, though the average *RMSE* reached 9.27° for EEG and 9.57° for EMG/EEG. In contrast, upon analyzing the results of modeling an LSTM with EMG as the input signal and setting the timesteps to 80, instead of 40, the model presented the lowest average *RMSE* (8.59°) of all signals, thus showing the best performance, with a standard deviation error of 2.17°, which approaches the average of all the standard deviation errors. Note that although the signal with the lowest average *RMSE* is EMG, the EEG and EMG/EEG presented performances that could be considered more precise than EMG, given that the corresponding standard deviation errors are lower and the differences with respect to the EMG estimation (8.59°) are about 0.68° and 0.98° greater than for the EMGs.

Turning to the influence of the number of timesteps for LSTM training, in the cases of EMG and EMG/EEG, the average *RMSE* decreased upon increasing from 40 to 80 timesteps, likely as a consequence of considering twice as much previous information. At the same time, this increased the estimation capability of the LSTM. An ANOVA analysis was also conducted to identify the combination (signal type and timestep) that best performed in terms of the elbow angle estimations (see Table 2). Results suggest that no particular combination works best,

so we propose using these results as a guide for selecting the combination that best fits each specific problem, especially when there is a dependence on the available signal, and considering the trade-off between variance and the expected *RMSE*.

With respect to the inter-subject analysis, it is clear that regardless of signal type and gender, increasing the number of timesteps from 40 to 80 improved, on most tests, the estimation performance of the LSTM model. This is consistent with the results presented for our intra-subject experiments and, as mentioned above, this is a consequence of considering more previous information when making the estimations. This is made possible by taking advantage of the LSTM's ability to store both long- and short-term relations. As seen in Tables 1 and 3, the best results were obtained when performing intra-subject tests, in contrast with the inter-subject tests. This is expected, considering that the intra-subject results correspond to the average of different model evaluations, where every model represents a different subject. On the contrary, when grouping by men or women, the RMSE increases considerably, as a consequence of the inter-subject variability that increments the complexity of the problem modeling. In addition, upon observing the results by gender, men presented lower average *RMSEs* than women in each signal type. This specific difference in performance of the EMG on gender could be due to the amount of force used by women, which is lower than that exerted by men [13]. Thus, when grouping the EMG data, the error increases due to the high inter-subject signal variability, accentuated by gender differences.

In general, regardless of the type of signal and number of timesteps, men had lower average *RMSEs* than women. In the case of EMG, this may be because men have higher neuromuscular activation than women [37]. With reference to the EEG data, Table 4 shows that there were significant differences in inter-subject performance between men and women when using EEG signals for the angular estimations since a p-value of 0.0027 was obtained. These differences are consistent with the state-of-the-art results presented by Cantillo et al., [38], who confirmed that gender produces significant differences in EEG signals when analyzing motor tasks.

When the features extracted from both EMG and EEG signals are appended, the LSTM models trained with those features present the best performances as the lowest average *RMSE* was achieved for both men and women (see Table 3). This could be interpreted as indicating that there are some combinations of features between EMG and EEG signals that allow the LSTM models to improve their performance for elbow angle estimations. This is supported by the data in Table 4, which shows significant differences, p-value < 0.01, between using the EEG signal and the combination of EEG/EMG signals for both men and women. Considering that the combination of EEG/EMG signals had a lower average RMSE than that reported by EEG, we consider convenient to use the combination of both signals rather than the EEG signal alone. Comparing this work with the state-of-the-art, Table 6 presents a comparison of the scores achieved in related works and our proposal. It is clear that our elbow flexion–extension estimations outperform those presented in the state-of the-art.

All comparisons consider that, even though other authors estimated others movements –such as forearm pronation-supination, shoulder abduction-adduction, using EMG, in the cases of [7,8] - or hand movements, considering EEG [11], we present only scores from elbow flexion–extension angle estimation from the EMG signal. Particularly, Akhtar et al. [8] studied 3 people with unilateral right trans-humeral amputations and targeted motor reinnervation obtaining an *RMSE* of 17.58° employing the LWPR as estimation method an 17.73° using the TDNN. Additionally, the most recent work found, Blana et al. [12], performs the elbow flexion–extension estimation using the LSTM as the estimation method, and the EMG and humerus acceleration as input signals. They reached an *RMSE* of 10.4°, while our work presents an *RMSE* of 8.69° using only the EMG as an input signal. It is pertinent to consider that for the LSTM configuration, Blana et al. [12], used 6 time-steps while we used 80 time-steps. It is important to note that we were unable to find any previous studies that used EEG signals with machine learning models which would have allowed us to make additional comparisons.

As far as subject-wise cross-validation concerns, as suggested by Little et al. [39] both record and subject-wise cross validation is presented in Tables 3 and 5, respectively. As can be seen on Table 5, there is an increase on the error estimation of every subject-wise experiment compared with the record-wise, which is a direct consequence of testing with instances from an unknown subject. It is worth noting two things, first, the best performances reported for subject-wise experiments corresponds to those using 40 timesteps in contrast with the 80 timesteps used in record-wise experiments. Second, for men, the error increase only 3.47° which is consistent with record-wise results and the state-of-the-art as mentioned before by Clark et. al [37] and Cantillo-Negrete et. al [38] who found gender differences on EMG and EEG signals.

Regarding the signal pre-processing employed in this work, it is important to mention that an additional experiment was performed in which ICA was used to remove artifacts from the signals, which were then tested with the proposed processing chain. We determined, however, that the results obtained after ICA pre-processing did not improve the findings presented. We believe that filter banks obtained from the wavelet transform used to extract features from the EEG signals were sufficient to prevent artifacts while simultaneously maintaining the relevant information. As mentioned above, the wavelet selected was of the 5^{th} order from the Daubechies family (db5).

To summarize, observations of the results obtained from the intra-subject data, in general, indicate that the best performances (lowest average *RMSE* and highest R^2 coefficient) were obtained with the methodology we propose. The best results were achieved using the EMG signals with an *RMSE* $= 8.59°$, followed by the EEG and EMG/EEG results at 9.44° and 9.53°, respectively. In contrast, if the goal is to perform a model adopted to one gender, then our work suggests training an LSTM model that also sets the timesteps to 80 or 40 but that uses EMG/EEG as the input signal for either women or men alone. In Table 2 it is shown that there are no significant differences between using a particular type of signal considering intra-subject data, therefore, when it is necessary to train a model for a particular subject, any type of signal can be used indiscriminately. In contrast, if the goal is to perform a model adopted to one gender, then our work suggests training an LSTM model that also sets the timesteps to 80 or 40 but that uses EMG/EEG as the input signal for either women or men alone.

5. Conclusion

In this work, we successfully estimated the angular value of the elbow joint based on EMG and EEG signals, using an LSTM artificial neural network. The recurrent network was selected because it is ideal for modeling sequential data. Hence, when using EMG signals it is better to train one network per person, while if a generalized model is required for either women or men, training an LSTM model using the combination of EMG/EEG signals will provide good performance. Also, our work agrees with the results of Blana et al. [12], showing that LSTM networks could be the most promising model for the development of neural controllers for upper limb prostheses.

CRediT authorship contribution statement

Valeria del C. Silva-Acosta: Methodology, Software, Validation, Formal analysis, Investigation, Resources, Writing - original draft, Writing - review & editing, Visualization. **Israel Roman-Godinez:** Conceptualization, Methodology, Validation, Formal analysis, Investigation, Writing - original draft, Writing - review & editing, Visualization, Supervision, Project administration. **Sulema Torres-Ramos:** Methodology, Validation, Formal analysis, Investigation, Writing - original draft, Writing - review & editing, Visualization, Supervision, Project administration. **Ricardo A. Salido-Ruiz:** Conceptualization,

Methodology, Validation, Formal analysis, Investigation, Writing - original draft, Writing - review & editing, Visualization, Supervision, Project administration.

Declaration of Competing Interest

The authors declare that they have no known competing financial interests or personal relationships that could have appeared to influence the work reported in this paper.

Acknowledgment

The author, V. C. Silva-Acosta, thanks CONACyT for the scholarship granted to pursue her postgraduate studies.

Appendix A. Supplementary data

Supplementary data associated with this article can be found, in the online version, at https://doi.org/10.1016/j.bspc.2021.102950.

References

[1] World Health Organization, World report on disability 2011, World Health Organization, 2011.
[2] P. Maduri, H. Akhondi, Upper Limb Amputation, StatPearls Publishing (2020). URL: http://www.ncbi.nlm.nih.gov/pubmed/31082006.
[3] M.P. Fahrenkopf, N.S. Adams, J.P. Kelpin, V.H. Do, Hand amputations, Eplasty 18.
[4] T. Kawase, T. Sakurada, Y. Koike, K. Kansaku, A hybrid BMI-based exoskeleton for paresis: EMG control for assisting arm movements, Journal of Neural Engineering 14 (1) (2017) 16015.
[5] D. Shin, J. Kim, Y. Koike, A myokinetic arm model for estimating joint torque and stiffness from EMG signals during maintained posture, Journal of Neurophysiology 101 (1) (2009) 387–401.
[6] T.D. Lalitharatne, A. Yoshino, Y. Hayashi, K. Teramoto, K. Kiguchi, Toward EEG control of upper limb power-assist exoskeletons: A preliminary study of decoding elbow joint velocities using EEG signals, in: 2012 International Symposium on Micro-NanoMechatronics and Human Science, MHS 2012, vol. 10, 2012, pp. 421–424.
[7] D. Blana, T. Kyriacou, J.M. Lambrecht, E.K. Chadwick, Feasibility of using combined EMG and kinematic signals for prosthesis control: A simulation study using a virtual reality environment, Journal of Electromyography and Kinesiology 29 (2016) 21–27.
[8] A. Akhtar, N. Aghasadeghi, L. Hargrove, T. Bretl, Estimation of distal arm joint angles from EMG and shoulder orientation for transhumeral prostheses, Journal of Electromyography and Kinesiology doi:10.1016/j.jelekin.2017.06.001.
[9] C. Grech, T. Camilleri, M. Bugeja, Using neural networks for simultaneous and proportional estimation of upper arm kinematics, in: 2017 25th Mediterranean Conference on Control and Automation, MED, 2017 (2017), pp. 247–252, https://doi.org/10.1109/MED.2017.7984126.
[10] D.S. Bandara, J. Arata, K. Kiguchi, Towards control of a transhumeral prosthesis with EEG signals, Bioengineering 5 (2) (2018) 10–16.
[11] K. Chen, Y. Zhang, Z. Zhang, Y. Yang, H. Ye, Trans humeral prosthesis based on sEMG and SSVEP-EEG Signals, IEEE International Conference on Robotics and Biomimetics, ROBIO 2019 – (18) (2019) 2665–2670.
[12] C.R. Day, E.K. Chadwick, D. Blana, A comparative evaluation of time-delay, deep learning and echo state neural networks when used as simulated transhumeral prosthesis controllers, in: 2020 International Joint Conference on Neural Networks (IJCNN), IEEE, 2020, pp. 1–7.
[13] A.E.J. Miller, J. MacDougall, M. Tarnopolsky, D. Sale, Gender differences in strength and muscle fiber characteristics, European Journal of Applied Physiology and Occupational Physiology 66 (3) (1993) 254–262.
[14] J.L. Semmlow, B. Griffel, Biosignal and Medical Image Processing, CRC Press, 2014.
[15] D.C. Toledo-Pérez, J. Rodríguez-Reséndiz, R.A. Gómez-Loenzo, A study of computing zero crossing methods and an improved proposal for emg signals, IEEE Access 8 (2020) 8783–8790, https://doi.org/10.1109/ACCESS.2020.2964678.
[16] A. Phinyomark, P. Phukpattaranont, C. Limsakul, Feature reduction and selection for EMG signal classification, Expert Systems with Applications 39 (8) (2012) 7420–7431, https://doi.org/10.1016/j.eswa.2012.01.102.
[17] B. Hudgins, P. Parker, R. Scott, A new strategy for multifunction myoelectric control, IEEE Transactions on Biomedical Engineering 40 (1) (1993) 82–94, https://doi.org/10.1109/10.204774.
[18] R.J.E. Merry, M. Steinbuch, Wavelet theory and applications. Eindhoven University of Technology, Department of Mechanical Engineering, Tech. rep. (2005).
[19] P. Ofner, A. Schwarz, J. Pereira, D. Wyss, R. Wildburger, G.R. Muller-Putz, Attempted arm and hand movements can be decoded from low-frequency eeg from persons with spinal cord injury, Scientific Reports 9 (1) (2019) 1–15, https://doi.org/10.1038/s41598-019-43594-9.
[20] G. Chen, A Gentle Tutorial of Recurrent Neural Network with Error Backpropagation (2016) 1–10. URL: http://arxiv.org/abs/1610.02583.
[21] Z. Cui, R. Ke, Y. Wang, Deep Bidirectional and Unidirectional LSTM Recurrent Neural Network for Network-wide Traffic Speed Prediction (2018) 1–11. URL: http://arxiv.org/abs/1801.02143.
[22] J. Han, M. Kamber, J. Pei, Data mining concepts and techniques third edition., 3rd Ed., vol. 53, The Morgan Kaufmann Series in Data Management Systems., 2013. doi:10.1017/CBO9781107415324.004.
[23] T. Tjur, Coefficients of determination in logistic regression models–a new proposal: The coefficient of discrimination, The American Statistician 63 (4) (2009) 366–372.
[24] A. Hazra, Using the confidence interval confidently, Journal of Thoracic Disease 9 (10) (2017) 4125.
[25] Y. Li, W. Zhang, Q. Zhang, N. Zheng, Transfer learning-based muscle activity decoding scheme by low-frequency semg for wearable low-cost application, IEEE Access 9 (2021) 22804–22815.
[26] H. Chen, Y. Zhang, Z. Zhang, Y. Fang, H. Liu, C. Yao, Exploring the relation between emg sampling frequency and hand motion recognition accuracy, in: 2017 IEEE International Conference on Systems, Man, and Cybernetics (SMC), IEEE, 2017, pp. 1139–1144.
[27] J.G. Proakis, D.G. Manolakis, Digital signal processing, PHI Publication: New Delhi, India.
[28] Triwiyanto, Herianto, O. Wahyunggoro, H.A. Nugroho, Quantitative relationship between feature extraction of sEMG and upper limb elbow joint angle, Proceedings – 2016 International Seminar on Application of Technology for Information and Communication, ISEMANTIC 2016 (2017) 44–50 doi:10.1109/ISEMANTIC.2016.7873808.
[29] J.A.F. Ernando, D.E.S. Aa, Clasificación de Señales Cerebrales Durante la Ejecución de Actividad Motora Imaginaria., LACCEI (2011) 1–10.
[30] J.-H. Kim, R. Chavarriaga, J. d. R. Millán, S.-W. Lee, Three-dimensional upper limb movement decoding from eeg signals, in: 2013 International Winter Workshop on Brain-Computer Interface (BCI), IEEE, 2013, pp. 109–111.
[31] A. Vourvopoulos, S.B.i. Badia, Usability and cost-effectiveness in brain-computer interaction: is it user throughput or technology related?, in: Proceedings of the 7th Augmented Human International Conference, 2016, 2016, pp. 1–8.
[32] S. Sreeja, J. Rabha, D. Samanta, P. Mitra, M. Sarma, Classification of motor imagery based eeg signals using sparsity approach, in: International Conference on Intelligent Human Computer Interaction, Springer, Cham, 2017, pp. 47–59.
[33] S. Saeb, L. Lonini, A. Jayaraman, D.C. Mohr, K.P. Kording, The need to approximate the use-case in clinical machine learning, Gigascience 6 (5) (2017) gix019.
[34] A. Dehghani, T. Glatard, E. Shihab, Subject cross validation in human activity recognition, arXiv preprint arXiv:1904.02666.
[35] A. Seth, J.L. Hicks, T.K. Uchida, A. Habib, C.L. Dembia, J.J. Dunne, C.F. Ong, M. S. DeMers, A. Rajagopal, M. Millard, et al., Opensim: Simulating musculoskeletal dynamics and neuromuscular control to study human and animal movement, PLoS Computational Biology 14 (7) (2018), e1006223.
[36] E.K. Chadwick, D. Blana, R.F. Kirsch, A.J. van den Bogert, Real-time simulation of three-dimensional shoulder girdle and arm dynamics, IEEE Transactions on Biomedical Engineering 61 (7) (2014) 1947–1956.
[37] B.C. Clark, T.M. Manini, D.J. The, N.A. Doldo, L.L. Ploutz-Snyder, Gender differences in skeletal muscle fatigability are related to contraction type and emg spectral compression, Journal of Applied Physiology 94 (6) (2003) 2263–2272.
[38] J. Cantillo-Negrete, R.I. Carino-Escobar, P. Carrillo-Mora, T.B. Flores-Rodríguez, D. Elias-Vinas, J. Gutierrez-Martinez, Gender differences in quantitative electroencephalogram during a simple hand movement task in young adults, Revista de Investigación Clinica 68 (5) (2017) 245–255.
[39] M.A. Little, G. Varoquaux, S. Saeb, L. Lonini, A. Jayaraman, D.C. Mohr, K.P. Kording, Using and understanding cross-validation strategies. Perspectives on Saeb et al., GigaScience 6 (5), gix020. arXiv:https://academic.oup.com/gigascience/article-pdf/6/5/gix020/25514479/gix020.pdf, doi:10.1093/gigascience/gix020. URL: doi: 10.1093/gigascience/gix020.